Characterization of phenylalanine ammonia-lyase genes facilitating flavonoid biosynthesis from two species of medicinal plant *Anoectochilus*

Lin Yang [1], **Wan-Chen Li** [2], **feng-ling Fu** [2], **Jingtao Qu** [2], **Fuai Sun** [2], **Haoqiang Yu** [Corresp., 2], **Juncheng Zhang** [Corresp. 1]

[1] Sanming University, Medical Plant Exploitation and Utilization Engineering Research Center Fujian Province University, Sanming, China

[2] Sichuan Agricultural University, Maize Research Institute, Chengdu, China

Corresponding Authors: Haoqiang Yu, Juncheng Zhang
Email address: yhq1801@sicau.edu.cn, 19900204@fjsmu.edu.cn

Background. *Anoectochilus roxburghii* and *Anoectochilus formosanus*, belong to the *Anoectochilus* genus, have been used for Chinese herbal drugs as well as health food. Phenylalanine ammonia-lyase (PAL), the key enzyme in primary metabolism and phenylpropanoid metabolism, produces secondary metabolites (flavonoids) in plants, which are beneficial for the biosynthesis of phenylpropanoid metabolites. **Methods.** The *PAL* genes were cloned from *A. formosanus* and *A. roxburghii* according to our previous transcriptomic analysis. The *PALs* were introduced into pCAMBIA2300-35S-PAL-eGFP to generate 35S-PAL-eGFP. The constructs were further used for subcellular localization and transgenic *Arabidopsis*. The expression of *AfPAL* and *ArPAL* under precursor substance (L-Phe), NaCl, UV, and red-light were analyzed by real-time quantitative PCR (RT-qPCR). **Results.** *AfPAL* and *ArPAL* , encoding 2,148 base pairs, were cloned from *A. formosanus* and *A. roxburghii*. The subcellular localization showed that the ArPAL and AfPAL were both localized in the nucleus with GPF. Quantitative RT-PCR analysis indicated that the *ArPAL* and *AfPAL* genes function in the phenylalanine pathway as well as response to induced conditions. Overexpression of the *AfPAL* and *ArPAL* could increase flavonoids and anthocyanin content in the transgenic *Arabidopsis*. **Discussion.** The results suggest that *AfPAL* and *ArPAL* play a crucial role in the flavonoid biosynthesis in *Anoectochilus*. Also, our study provides new insights into the enrichment of secondary metabolites of traditional Chinese medicines *A. formosanus* and *A. roxburghii*， which can improve their medicinal active ingredients and be used for drug discovery in plants.

Characterization of phenylalanine ammonia-lyase genes facilitating flavonoid biosynthesis from two species of medicinal plant *Anoectochilus*

Lin Yang[1], Wanchen Li[2], Fengling Fu[2], Jingtao Qu[2], Fuai Sun[2], Haoqiang Yu[2], Juncheng Zhang[1]

[1] Medical Plant Exploitation and Utilization Engineering Research Center Fujian Province University, Sanming University, Sanming, Fujian, China
[2] Maize Research Institute, Sichuan Agricultural University, Chengdu, Sichuan, China

Corresponding Author:
Juncheng Zhang[1]
Jingdong Road No.25, Sanming, Fujian, China, 365004
Email address: 19900204@fjsmu.edu.cn
Haoqiang Yu[2]
Huimin Road No.211, Chengdu, Sichuan, China, 611130
Email address: yhq1801@sicau.edu.cn

Abstract

Background. *Anoectochilus roxburghii* and *Anoectochilus formosanus*, belong to the *Anoectochilus* genus, have been used for Chinese herbal drugs as well as health food. Phenylalanine ammonia-lyase (PAL), the key enzyme in primary metabolism and phenylpropanoid metabolism, produces secondary metabolites (flavonoids) in plants, which are beneficial for the biosynthesis of phenylpropanoid metabolites.

Methods. The *PAL* genes were cloned from *A. formosanus* and *A. roxburghii* according to our previous transcriptomic analysis. The *PALs* were introduced into pCAMBIA2300-35S-PAL-eGFP to generate 35S-PAL-eGFP. The constructs were further used for subcellular localization and transgenic *Arabidopsis*. The expression of *AfPAL* and *ArPAL* under precursor substance (L-Phe), NaCl, UV, and red-light were analyzed by real-time quantitative PCR (RT-qPCR).

Results. *AfPAL* and *ArPAL* , encoding 2,148 base pairs, were cloned from *A. formosanus* and *A. roxburghii*. The subcellular localization showed that the ArPAL and AfPAL were both localized in the nucleus with GPF. Quantitative RT-PCR analysis indicated that the *ArPAL* and *AfPAL* genes function in the phenylalanine pathway as well as response to induced conditions. Overexpression of the *AfPAL* and *ArPAL* could increase flavonoids and anthocyanin content in the transgenic *Arabidopsis*.

Discussion. The results suggest that *AfPAL* and *ArPAL* play a crucial role in the flavonoid biosynthesis in *Anoectochilus*. Also, our study provides new insights into the enrichment of secondary metabolites of traditional Chinese medicines *A. formosanus* and *A. roxburghii*, which can improve their medicinal active ingredients and be used for drug discovery in plants.

Introduction

Anoectochilus is a specie of orchidaceae family and possesses various pharmaceutical constituents, which plays an important role in cancer treatment (Lang et al., 1999; Shyur et al., 2004; Yang et al., 2014; Yu et al., 2017). Currently, *Anoectochilus formosanus* and *Anoectochilus roxburghii* which are obviously different in morphology, are both widely used in cultivation or tissue culture for rapid propagation (Figure 1, Du et al., 2000; Shiau et al., 2002; Zhang et al., 2015). However, the synthesis and catabolism of the pharmaceutical constituents including flavonoid, polysaccharides, glycoside derivative kinsenoside, and steroids in the cultivated *Anoectochilus* is primary and produced by secondary metabolites (Dai et al., 2009), which is different from wild plants (Du et al., 2000). It's significant to promote the accumulation of flavonoids of two medicinal plants *Anoectochilus* in artificial cultivation or tissue culture. Phenylalanine ammonia-lyase (PAL, EC 4.3.1.24) is essential for connecting of primary and phenylpropanoid metabolism in plants. The PAL controls the speed of the first step in the biosynthesis of phenylpropanoid metabolites, the nonoxidative deamination of phenylalanine to trans-cinnamic acid and ammonia (Lois et al., 1989; Nugroho et al., 2002). Subsequently, phenylpropanoids will produce several secondary metabolites, such as flavonoid, phytohormone, anthocyanin, lignin, phytoalexin, and benzoic acid (Figure S1, Jorrin & Dixon, 1990; Jin et al., 2013). To date, the *PAL* genes have been cloned and characterized by homologous amplification and rapid amplification of cDNA ends (RACE) from variant medicinal plants, such as *Dendrobium* (Jin et al., 2013), *Artemisia annua* (Zhang et al., 2016), *Fagopyrum tataricum* (Li et al., 2012) and *Ginkgo biloba* (Cheng et al., 2005). However, genome information is not available for homologous amplification for any of the *Anoectochilus* species. The expression of the *PAL* gene and activity of the PAL protein are found to be responsive to light quality, salinity, drought, wounding, and related to secondary metabolites accumulation in other plants (Nakazawa et al., 2001; Zhang et al., 2012; Zhang et al., 2016).

Given the importance of *A. formosanus*, *A. roxburghii,* and the active compounds in these *Anoectochilus*, it is essential for functional studies into the medicinal plant. In the present study, the *PAL* genes were cloned from *A. formosanus* and *A. roxburghii* according to our transcriptional analysis. After bioinformatics analysis, the expression of the *AfPAL* and *ArPAL* genes in response to precursor substance (L-Phe), NaCl, UV, and red-light were detected by real-time quantitative PCR (RT-qPCR), respectively. The subcellular localization and heterologous expression of the *AfPAL* and *ArPAL* genes were performed. These results demonstrate that the *AfPAL* and *ArPAL* genes play an important role in flavonoids biosynthesis in *Anoectochilus*.

Materials & Methods

Sample preparation

The seedlings of *A. formosanus* and *A. roxburghii* were surface sterilized using 10% NaClO for 5 mins and plated onto MS medium in a chamber under a 12 h light / 12 h dark at 28 °C and 60-80% humidity condition. The 4-month-old seedlings were transferred into a plastic mesh grid for

aquaculture with Hoagland's nutrient solution. The seedlings were transferred into a plastic mesh grid for aquaculture. Phe and NaCl were added into the nutrient solution with a final concentration of 4 mg/L and 100 mmol/L. The seedlings were also transplanted into plastic pots cultivated with nutritional soil and vermiculite (3:1), and then induced under a 253.7 nm UV and 650 nm red light. The leaves samples were collected from each replicate at 0 h (control), 0.5 h, 1 h, 2 h, 4 h, 8 h, 12 h of the Phe, NaCl, UV, and red-light induction, respectively. The RNA was extracted with Qiagen RNeasy plant mini kit (Qiagen, China), following cDNA were revere transcribed by PrimeScript RT reagent Kit (Takara China).

Cloning of the *PAL* Gene

The open reading frame (ORF) of the *AfPAL* and *ArPAL* gene from cDNA were amplified based on the annotation of RNA-seq by specific primers (5'-ATGGACCATGCTAGGGAGAACG-3'/5'-CTAGCAAATAGGGAGAGGAGCTTCA-3') (http://www.premierbiosoft.com/primerdesign/) The amplified fragments were purified using Universal DNA Purification Kit (Tiangen, China), added dATP in the tail of sequences using the TaKaRa TaqTM (TakaRa, China), cloned into pMD19-T vector (TakaRa, China), and sequenced by Shanghai Sangon Biotech Co., Ltd (China).

Bioinformatic analysis

The sequencing of the *AfPAL* and *ArPAL* genes were aligned for gene structure using blast on NCBI website (http://www.ncbi.nl- m.nih.gov) and used for the analysis of physical and chemical properties, secondary structure, functional domains, and genetic structure of the putative proteins by using ProtParam (http://web.expasy.org/protparam), GOR IV (http://npsa-pbil.ibcp.fr/cgi-bin/npsa_automat.pl?page=npsa_gor4.html), TMHMM Server v. 2.0 (http://www.cbs.dtu.dk/services/TMHMM-2.0/) and SWISS-MODEL (https://swissmodel.expasy.org/) software or databases, respectively. Phylogenetic analysis among the putative amino acid sequences of the AfPAL and ArPAL proteins at the NCBI database were analyzed using the method of maximum likelihood of 1000 bootstrap replicates by using MEGA7.0 software (https://www.megasoftware.net/). The evolutionary distances were computed by using the Poisson correction method.

Vector construction

A pair of homologous arms (the lowercase bases) primers (5'-catttggagaggacagggtacccgggATGGACCATGCTAGGGAGAACG-3'/5'-tcgcccttgctcaccatggtactagtGCAAATAGGGAGAGGAGCTTCA-3') was designed to amplify the ORFs of the *AfPAL* and *ArPAL* genes without termination codon for homologous recombination. The amplified PCR were inserted into the expression vector pCAMBIA2300 using CloneExpress One Step Cloning Kit (Vazyme, China) respectively, to generate a set of expression vectors bearing fusion genes between the *AfPAL* and *ArPAL* genes and the enhanced green fluorescent protein gene *eGFP*, *AfPAL*/*ArPAL-eGFP* (Figure S2).

RT-qPCR

A pair of specific primers (5'- AGCAAGATTACGCCTTGCCT-3'/5'-AAGGCCTCTACTGCGTTGAC-3') was designed to amplify a 152 bp fragment of the *AfPAL* and *ArPAL* genes. Another pair of specific primers (5'-CGGGCATTCACGAGACCAC-3'/5'-AATAGACCCTCCAATCCAGACACT-3') was designed to amplify a 221 bp fragment of the internal reference gene *Actin2* (Zhang et al., 2012). The PCR reaction was conducted on SsoFast EvaGreen Supermix (Bio-Rad, USA) according to the protocol. The $2^{-\Delta\Delta CT}$ method was used to normalize the expression between the internal reference and the *PAL* genes (Livak and Schmittgen, 2001). The data was further analyzed by IBM-SPSS software (http://www-01.ibm.com/software/analytics/spss/).

Subcellular localization

The 35S-PAL-eGFP recombined vectors were attached onto gold particles (φ = 60 μm) by the spermidine and $CaCl_2$ method with 35S-eGFP empty vector as control (Yu et al., 2018). Onion bulbs were surface sterilized with 75% (v/v) ethanol. The healthy fourth to sixth scales were cut into 2 × 2 cm, cultured on Murashige and Skoog's (MS) medium for 4-6 h under dark at28 °C, and then bombarded using helium biolistic gun (Bio-Rad, USA), incubated for 24 h at 28 °C under dark condition (Sun et al., 2021). The fluorescence signal was detected by a confocal microscope (Nikon, Japan; Yang et al., 2019).

Transformation of *Arabidopsis*

The pCAMBIA2300-35S-PAL-eGFP plasmid was mobilized into *Agrobacterium tumefaciens* strain EHA105 and used to transform wild-type *Arabidopsis* as described (Sun et al., 2020). The transformed lines were screened on 1/2 MS medium supplemented with 35 mg / L kanamycin (Sigma, USA). The homozygous lines were identified by PCR amplification with specific primers (5'- CATTTGGAGAGGACAGGGTACC-3'/5'-CTAGCAAATAGGGAGAGGAGCTTCA-3') for Af*PAL* and *ArPAL*.

Flavonoid quantification

The leaf of T_3 lines and wild type were dried and ground to be extracted by 95% alcohol in an ultrasonic instrument at 25 °C for 0.5h. The extracts were filtered, and the residues were dissolved in 95% alcohol. The residues were filtered again. The filtrates were combined, and solvents were removed under reduced pressure using the rotavapor R-210 (BUCHI, Switzerland) to yield the extract. The template samples were detected using the reagent color-developing method ($NaNO_2$-$Al(NO_3)_3$–NaOH). The above stock solutions 1 ml were added with 0.4 mL 5 % $NaNO_2$ for 5 min. The 10 % $Al(NO_3)_3$ 0.4 ml were added to the reaction. After standing for 5 min, 4 % NaOH 4 ml were used to color. The reactions were incubated for 20 min. The quantitative values were determined with a UV-1800 spectrophotometer at 420 nm. The content of total flavonoids was calculated as:

Content of flavonoids = $(A_{420} \times V) / (m \times d)$

Where, A_{420} was the absorbance at 420 nm, V repreents total volume of the extract, mM was the extraction quality from the leaf of each sample (1 g), d repreents the dilution multiple (Chen et al., 2007).

Anthocyanin measurement

The leaves of T_3 lines and wild type were pulverized to fine powder in liquid nitrogen, extracted with acidified (1% HCl) methanol, and incubated dark with shaking for 48 h. Later, it was centrifuged at 4000 g for 10 min following the protocol described by Tanaka et al. (1997). The supernatant was used to measure absorbance at 535 nm in a UV-1800 spectrophotometer. The anthocyanidin content was indicated by absorption value.

Results

Cloning the *AfPAL* and *ArPAL* genes.

Based on RNA-seq information, we designed the specific primers to amplify the *AfPAL* and *ArPAL. The* fragments of more than 2148 bp were amplified from the cDNA library of *A. formosanus* and *A. roxburghii*, respectively (Figure S3, MK387342 and MK387343). The constructs were verified by PCR and sequencing; the fragment from the cDNA of *A. formosanus* and *A. roxburghii* showed high homology to reported *PAL* bioinformatics-predicted sequences (Figure S4).

Proteins sequence analysis

The amino acid sequences of the AfPAL and ArPAL proteins were highly homologous with that from *Phalaenopsis equestris* (XP_020579635.1) and *Dendrobium huoshanense* (Figure 2 and 3). The AfPAL and ArPAL proteins both contained 715 amino acids with a molecular weight 77.4 kDa, isoelectric point pI 6.18 and 6.26, grand average of hydropathicity (GRAVY) -0.104 and -0.103. The predicted secondary structure of these two proteins contained 48.53% and 48.67% α-helices, 10.07% and 9.79% extended strands, 41.40% and 41.54% random coils, respectively. Their three-dimensional structural model contained all the α-helices, extended strands, and random coils (Figure S5). Most of these properties of the AfPAL and ArPAL proteins were similar to the PePAL of *Phalaenopsis equestris*.

Conserved domain and Phylogenetic relationship

The conserved domain of the phenylalanine and histidine ammonia lyase signature (GTITASGDLVPLSYIA) and the active site Ala-Ser-Gly tripeptide forming the MIO group (3,5-dihydro-5-methylene-4H-imidazole-4-one) were found in position 197-213 and 201-203, respectively. Meanwhile, the strictly conserved residues, Y109, L137, S202, N259, Q347, Y350, R353, F399, and Q487, were found in the AfPAL and ArPAL protein, respectively. Moreover, the deamination sites such as L-205, V-206, L-255, and A-256, catalytic active sites such as N-259, G-260, NDN (381-383 aa), H-395 and HNQDV (485-488 aa), and the possible phosphorylation site such as VAKRVLTF (542-549aa) were found in both AfPAL and ArPAL

(Figure 2). Multiple alignment and phylogenetic analysis showed that the putative AfPAL and ArPAL proteins were clustered into the same sub-group with the deposited functional PAL proteins of *Dendrobium huoshanense* (Figure 3), indicating that the PAL proteins from *A. formosanus* and *A. roxburghii* are members of the PAL family.

Relative expression level under induction

The expression of the *AfPAL* gene in the stem was highest, about twice than the leaf, and it was the 20 times than root from *A. formosanus* ($P \leqslant 0.05$; Figure 4). And the expression of the *ArPAL* gene in the root was similar to that of the stem, about 10 times higher than the leaf from *A. roxburghii* ($P \leqslant 0.05$; Figure 4). And the expression of the *PAL* gene was similar in root from *A. formosanus*, leaf, and stem from *A. roxburghii*. The expression was downregulated significantly in *A. formosanus* and *A. roxburghii,* and there was a valley value at 1 h in response to Phe stress at the beginning. Then, the expression was upregulated in *A. formosanus* and *A. roxburghii* after 1 h, and reached their peaks at 4h and 2h, respectively. Then the expression plummeted, only one-tenth or even less with the control (Figure 5A). Under the NaCl stress, the expression was upregulated significantly in the two species and reached their valleys at 2 h (15.24 times) and 0.5 h (4.77 times), respectively (Figure 5B). In response to the UV stress, the overall trend of the expression of the *PAL* genes was upregulated, and there was a peak value at 12 h and 8 h, respectively (54.49 times and 873.89 times, Figure 5C). The expression was downregulated significantly in *A. formosanus* and reached its valley at 1 h in response to red light stress. In contrast, it was changed but not regular in the *A. roxburghii* (Figure 5D).

Subcellular localization

The subcellular localization of the PAL proteins was analyzed using the GFP as a reporter in transient expression assays, and bacterial cells carrying PAL-GFP plasmids were infiltrated into epidermal cells of onion. Confocal microscopy images demonstrated that the PAL-eGFP fusion protein was specifically distributed in the nucleus, whereas GFP alone showed ubiquitous distribution in the whole cell (Figure 6).

Overexpression of the *PAL* genes

To investigate the function of *PAL*， the transgenic Arabidopsis of PALs were generated. In the T_1 generation, five positive plants of three lines (F1-3) transformed by gene *AfPAL* and two lines (R1-2) by *ArPAL* were screened on the selection medium. In the T_2 generation, these lines were a single copy insertion with a ratio of 3:1 between the transformed genes and wild-type *Arabidopsis* (Figure S6). In the T_3 generation, homozygous lines without segregation were identified on the selection medium. The specific PCR amplification confirmed the altered genes from F1-3 and R1-2(Figure S7). The flavonoid contents were significantly higher in lines F-2 and R-1, and the anthocyanin content was considerably higher in lines F-2, F-3, R-1, and R-2 (Figure 7). The results revealed that the *PAL* genes were successfully expressed in five

independent transgenic events. The flavonoids and anthocyanin contents in transgenic lines were higher than in wild-type.

Discussion

The ORFs of the cloned *AfPAL* and *ArPAL* genes and the amino acid sequences of their putative proteins were highly homologous with the *PAL* gene and its putative protein in *Dendrobium huoshanense* as well as *Phalaenopsis equestris* (Figure 2 and 3). The conserved domain of the phenylalanine, histidine ammonia-lyase signature, and the active site Ala-Ser-Gly tripeptide forming the MIO group was necessary for their function (Gao et al., 2008). All the active sites were highly conserved among the reported PAL proteins (Cheng et al., 2005; Gao et al., 2008; Jin et al., 2013; Li et al., 2012; Zhang et al., 2016).

In many other plants, the expression of the *PAL* genes showed organic specificity, and the expression level was correlated to their accumulation of flavonoids (Fukasawa-Akada et al., 1996; Jin et al., 2013; Leyva et al., 1992; Zhang et al., 2016). In this paper, RT-qPCR analysis revealed that the high expression of the *PAL* genes was found in the stem of *A. formosanus* and the root of *A. roxburghii* (Figure 4). However, their differential expression was responsive to four stress or induction treatments. This result implies the different tolerance of these two species in the activities of *PAL* (Figure 5). The expression of the *PAL* genes was intensely up-regulated in response to NaCl and UV (Figure 5B and 5C), which was consistent with observations of other plants under stress conditions (Bell et al., 2017; El et al., 2003; El-Shora, 2002; Fritzemeier et al., 1981; Song et al., 2009). The range of the differential expression of the *AfPAL* gene was more extensive than the *ArPAL* gene under NaCl stress, but the content of the *AfPAL* gene was less than the *ArPAL* gene, conversely. In response to Phe and red-light induction, the expression of the *PAL* gene was downregulated, excepting a few sharp peaks (Figure 5A and 5D). Similar results were found in other plants (Nakazawa et al., 2001; Bellini and Hillman, 1971; Edahiro et al., 2005; Heo et al., 2012). Therefore, it is preliminary concluded that the expression of the *PAL* gene is more sensitive to saline induction in *A. formosanus* than *A. roxburghii*, and the latter is probably more sensitive to UV induction.

Subcellular localization of PAL protein has been studied in different plants (Fukasawa-Akada et al., 1996; Herdt and Wiermann, 1978). The present study investigated the subcellular localization of PAL protein in a heterologous system (the chloroplast-free epidermal cells of onion) by confocal laser-scanning microscopical imaging of GFP fluorescence (Figure 6). Transient expression of the *PAL-eGFP* fusion protein in the onion was targeted to the nucleus. The nuclei of five tree species with respect to the presence of flavanols (Feucht et al., 2014). Flavonoids and at least two of the biosynthetic enzymes are located in the nucleus in several cell types in *Arabidopsis* (Saslowsky and Winkel-Shirley, 2005). The result might indicate a high association of PAL protein to the nucleus or nuclear membrane and raise the possibility of novel mechanisms of action for flavonoids.

In the overexpressing transgenic lines of *Arabidopsis thaliana*, the content of flavonoids and anthocyanin was significantly higher than those in wild-type control (Figure 7). The increased

contents of total flavonoids should be associated with the genetically modified anthocyanin metabolic pathway (Figure S1). In addition, the content of total flavonoids and anthocyanins was higher in the *Arabidopsis* lines transformed by the *ArPAL* gene than those of the *AfPAL*. This result suggests that the activities of the proteins encoded by *PAL* genes might be differential between these two species. The transgenic tobacco with the overexpression PAL gene was developed in response to infection by tobacco mosaic virus and necrotrophic pathogens (Pallas et al., 2010; Way et al., 2011). Many reports indicated its critical function in the secondary metabolism of these plants (Lois et al., 1989; Nugroho et al., 2002).

Conclusions

The AfPAL and ArPAL genes' expression showed organic specificity and the differential expression of the *PAL* genes in response to four treatments. The flavonoid metabolites of *Arabidopsis* transformed with *AfPAL,* and the *ArPAL* gene were increased, provided by the anthocyanin metabolic pathway. And the different effects of overexpressed *Arabidopsis* flavonoids were caused by different *Anoectochilus* of the *PAL* gene.

References

Bell SM, Wendt DJ, Zhang Y, Taylor TW, Long S, Tsuruda L, Zhao B, Laipis P, Fitzpatrick PA. 2017. Formulation and PEGylation optimization of the therapeutic PEGylated phenylalanine ammonia-lyase for the treatment of phenylketonuria. *Plos One* **12**: e0173269.

Bellini E, Hillman WS. 1971. Red and Far-Red Effects on Phenylalanine Ammonia-Lyase in Raphanus and Sinapis Seedlings Do Not Correlate with Phytochrome Spectrophotometry. *Plant Physiology* **47**: 668-671.

Chen LG, Ding L, Yu AM, Yang RL, Wang XP, Li JT, Jin HY, Zhang HQ. 2007. Continuous determination of total flavonoids in *platycladus orientalis* (L.) franco by dynamic microwave-assisted extraction coupled with on-line derivatization and ultraviolet-visible detection. *Anal Chiem Acta* **596**: 164-170.

Cheng SY, Du HW, Xu F, Cheng KS. 2005. Molecular cloning of phenylalanine ammonia-lyase in *Ginkgo biloba*. *Forest Research* **18**: 573-577.

Du XM, Sun NY, Irino N, Shoyama Y. 2000. Glycosidic constituents from in vitro *Anoectochilus formosanus*. *Chemical & Pharmaceutical Bulletin* **48**: 1803-1804.

Dai YJ, Shao MM, Hannaway D, Wang LL, Liang JP, Hu LN, Lu HF. 2009. Effect of *Thrips tabaci* on anatomical features, photosynthetic characteristics, and chlorophyll fluorescence of *Hypericum sampsonii* leaves. *Crop Protection* **28**: 327-332.

Edahiro JI, Nakamura M, Seki M, Furusaki S. 2005. Enhanced accumulation of anthocyanin in cultured strawberry cells by repetitive feeding of l-Phenylalanine into the medium. *Journal of Bioscience and Bioengineering* **99**: 43-47.

El GA, Wilson CL, Callahan AM. 2003. Induction of Chitinase, beta-1,3-Glucanase, and Phenylalanine Ammonia Lyase in Peach Fruit by UV-C Treatment. *Phytopathology* **93**: 349.

El-Shora HM. 2002. Properties of phenylalanine ammonia-lyase from marrow cotyledons. *Plant Science* **162**(1): 1-7.
Feucht W, Treutter D, Polster J. 2014. Flavanol binding of nuclei from *tree species*. *Plant Cell Reports* **22**: 430-436.
Fritzemeier KH, Kindl H. 1981. Coordinate induction by UV light of stilbene synthase, phenylalanine ammonia-lyase, and cinnamate 4-hydroxylase in leaves of vitaceae. Plantation **151**: 48-52.
Fukasawa-Akada T, Kung SD, Watson JC. 1996. Phenylalanine ammonia-lyase gene structure, expression, and evolution in Nicotiana. *Plant Molecular Biology* **30**: 711-722.
Gao S, Ouyang C, Wang S, Xu Y, Tang L, Chen F. 2008. Effects of salt stress on growth, antioxidant enzyme and phenylalanine ammonia-lyase activities in *Jatropha curcas* L. seedlings. *Plant Soil and Environment* **54**, 374-381.
Heo JW, Kang DH, Bang HS, Hong SG, Chun C, Kang KK. 2012. Early growth, pigmentation, protein content, and phenylalanine ammonia-lyase activity of red curled lettuces grown under different lighting conditions. *Korean Journal of Horticultural Science & Technology* 30: 6-12.
Herdt E, Wiermann R. 1978. Subcellular localization of enzymes of phenylpropanoid metabolism in another tapetum: Phenylalanine ammonia-lyase, cinnamic acid 4-hydroxylase, SAM: Caffeic acid 3-0-methyltransferase. Protoplasma **96**: 283-292.
Jin Q, Yao Y, Cai Y, Lin Y. 2013. Molecular Cloning and Sequence Analysis of a Phenylalanine Ammonia-Lyase Gene from *Dendrobium*. *Plos One* **8**: e62352.
Jorrin J, Dixon RA. 1990. Stress Responses in Alfalfa (Medicago sativa L.): II. Purification, characterization, and induction of phenylalanine ammonia-lyase isoforms from elicitor-treated cell suspension cultures. Plant Physiology **92**: 447-455.
Lang KY, Chen XQ, Luo YB, Zhu GH. 1999. Angiospermae, in The Editorial Board of Flora of China. (Eds.), Flora of China (Volume XVII). Science Press Beijing: 220-227.
Leyva A, Liang X, Pintor-Toro JA, Dixon RA, Lamb CJ. 1992. Cis-element combinations determine phenylalanine ammonia-lyase gene tissue-specific expression patterns. *Plant Cell* **4**: 263-271.
Li CL, Bai YC, Chen H, Zhao HX, Shao JR, Wu Q. 2012. Cloning, Characterization, and Functional Analysis of a Phenylalanine ammonia-lyase Gene (*FtPAL*) from *Fagopyrum tataricumgaertn*. *Plant Molecular Biology Reporter* **30**: 1172-1182.
Livak KJ, Schmittgen TD. 2001. Relative gene expression data was analyzed using real-time quantitative PCR and the $2^{-\Delta\Delta CT}$ method. *Methods* **25**(4): 402-408
Lois R, Dietrich A, Hahlbrock K, Schulz W. 1989. A phenylalanine ammonialyaseammonia-lyase gene from parsley: structure, regulation, and identification of elicitor and light responsive cis-acting elements. EMBO Journal **8**: 1641-1648.
Nakazawa A, Nozue M, Yasuda H, Takeba G, Kubo H. 2001. Expression Pattern and Gene Structure of Phenylalanine Ammonia-Lyase in *Pharbitis nil*. *Journal of Plant Research* **114**: 323-328.

Nugroho LH, Verberne MC, Verpoorte R. 2002. Activities of enzymes involved in the phenylpropanoid pathway in constitutively salicylic acid-producing tobacco plants. Plant Physiology and Biochemistry **40**: 755-760.

Pallas JA, Paiva NL, Chris L, Dixon R. 2010. Tobacco plants epigenetically suppressed in phenylalanine ammonia-lyase expression do not develop systemic acquired resistance in response to infection by tobacco mosaic virus. *Plant Journal* **10**: 281-293.

Saslowsky D, Winkel-Shirley B. 2005. Nuclear localization of flavonoid enzymes in *Arabidopsis* roots. *Journal Of Biological Chemistry* **280**: 23735-23740.

Shiau YJ, Sagare AP, Chen UC, Yang SR, Tsay HS. 2002. Conservation of Anoectochilus formosanus Hayata by artificial cross-pollination and in vitro culture of seeds. *Botanical Bulletin of Academia Sinica* **43**: 123-130.

Shyur LF, Chen CH, Lo CP. Wang SY, Kang PL, Sun SJ, Chang CA, Tzeng CM, Yang NS. 2004. Induction of Apoptosis in MCF-7 Human Breast Cancer Cells by Phytochemicals from *Anoectochilus formosanus*. Journal of Biomedical Science **11**: 928-939.

Song J, Wang Z. 2009. Molecular cloning, expression, and characterization of a phenylalanine ammonia-lyase gene (SmPAL1) from Salvia miltiorrhiza. *Molecular Biology Reports* **36**: 939-952.

Sun F, Yu H, Qu J, Cao Y, Ding L, Feng W, Khalid MH Bin, Li W, Fu F. 2020. Maize ZmBES1/BZR1-5 Decreases ABA Sensitivity and Confers Tolerance to Osmotic Stress in Transgenic *Arabidopsis*. *International Journal of Molecular Sciences* **21**: 996.

Sun F, Ding L, Feng W, Cao Y, Lu F, Yang Q, Li W, Lu Y, Shabek N, Fu F, Yu H. 2021. Maize transcription factor ZmBES1/BZR1-5 positively regulates kernel size. *Journal of Experimental Botany* **72**(5).

Tanaka A, Tano S, Chantes T, Yokota Y, Shikazono N, Watanabe H. 1997. A new *Arabidopsis* mutant induced by ion beams affects flavonoid synthesis with spotted pigmentation in testa. Genes & Genetic Systems **72**: 141-148.

Way HM, Birch RG, Manners JM. 2011. A comparison of individual and combinedl-phenylalanine ammonia lyase and cationic peroxidase transgenes for engineering resistance in tobacco to necrotrophic pathogens. *Plant Biotechnology Reports* **5**: 301-308.

Yang LC, Hsieh CC, Lu TJ, Lin WC. 2014. Structurally characterized arabinogalactan from *Anoectochilus formosanus* as an immuno-modulator against CT26 colon cancer in BALB/c mice. *Phytomedicine* **21**: 647-655.

Yang L, Zhang JC, Qu JT, He G, Yu HQ, Li WC, Fu FL. 2019. Expression response of chalcone synthase gene to inducing conditions and its effect on flavonoids accumulation in two medicinal species of *Anoectochilus*. *Scientific Reports* **9**: 20171.

Yu H, Feng W, Sun F, Zhang YY, Qu JT, Liu B, Lu F, Yang L, Fu F, Li W. 2018. Cloning and characterization of BES1/BZR1 transcription factor genes in maize. Plant Growth Regulation 86:235–249.

Yu X, Lin S, Zhang J, Huang L, Yan H, Li S. 2017. Purification of polysaccharide from artificially cultivated *Anoectochilus roxburghii*(wall.) Lindl. by high-speed counter current chromatography and its antitumor activity. Journal of Separation Science **40**: 4338-4346.

Zhang G, Zhao M, Song C, Luo A, Bai J, Guo S. 2012. Characterization of reference genes for quantitative real-time PCR analysis in various tissues of *Anoectochilus roxburghii*. *Molecular Biology Reports* **39**: 5905-5912.

Zhang JG, Liu Q, Liu ZL, Li L, Yi LT. 2015. Antihyperglycemic activity of *Anoectochilus roxburghii* polysaccharose in diabetic mice induced by high-fat diet and streptozotocin. *Journal of Ethnopharmacology* **164**: 180-185.

Zhang WW, Li JB, Xu F, Tang Y, Hua C, Cao FL. 2016. Isolation and characterization of a phenylalanine ammonia-lyase gene (PAL) promoter from *Ginkgo biloba* and its regulation of gene expression in transgenic tobacco plants. *Rsc Advances* **6**: 28927-28936.

Zhang Y, Fu X, Hao X, Zhang L, Wang L, Qian H, Zhao J. 2016. Molecular cloning and promoter analysis of the specific salicylic acid biosynthetic pathway gene phenylalanine ammonia-lyase (*AaPAL1*) from *Artemisia annua*. *Biotechnology and Applied Biochemistry* **63**: 514-524.

Figure 1

Figure 1 The morphological characteristics of *A. formosanus* and *A. roxburghii*.

A and B represent *A. formosanus* and A. roxburghii; 1, 2 and 3 represents complete stool, leaf and stem; The leaf and stems of *A. formosanus* were white and pink, while those of *A. roxburghii* were golden yellow and green.

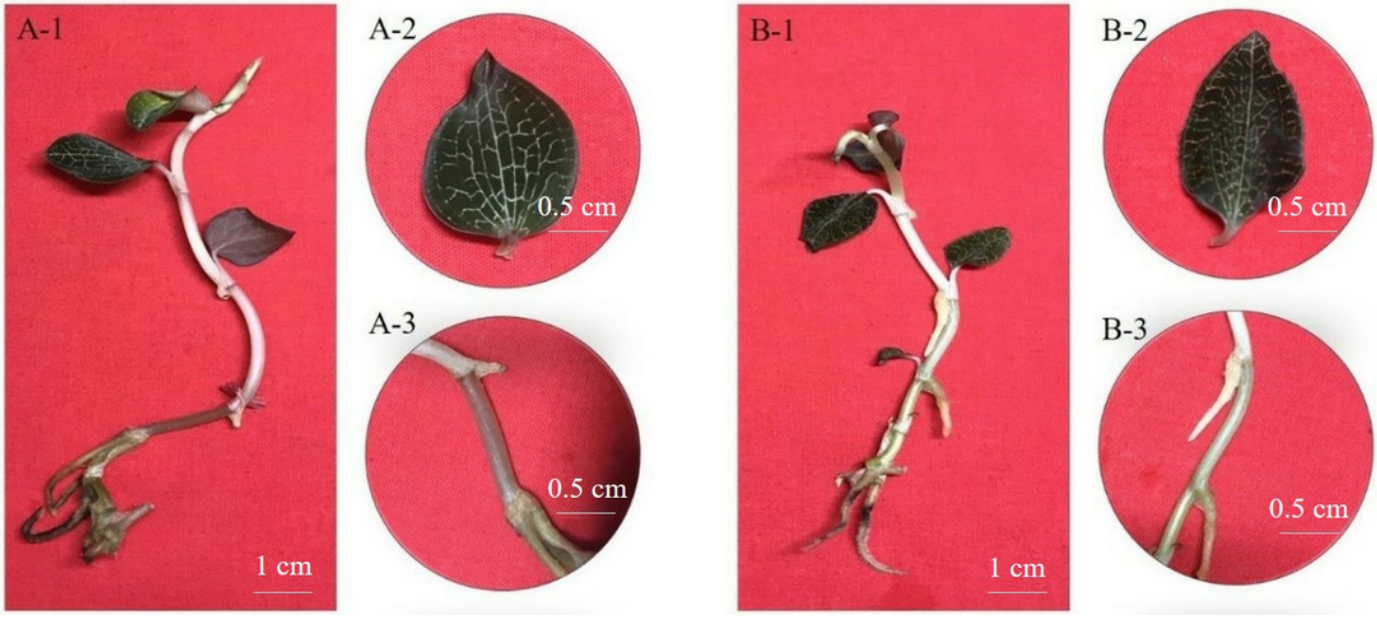

Figure 2

Figure 2 The structural functional domain of the PAL genes among *A. formosanus*, *A. roxburghii* and *Phalaenopsis equestris*.

Identical and conserved amino acid residues are denoted by black (100%), gray (66.6%) and white (0%) backgrounds, respectively. The boxes with solid line represent the phenylalanine and histidine ammonia lyase signature, the boxes with dotted line represent the possible phosphorylation sites, the asterisks represent the active sites, the solid dots represent strictly conserved residues, the circles represent the deamination sites and sharp corners represent the catalytic active sites.

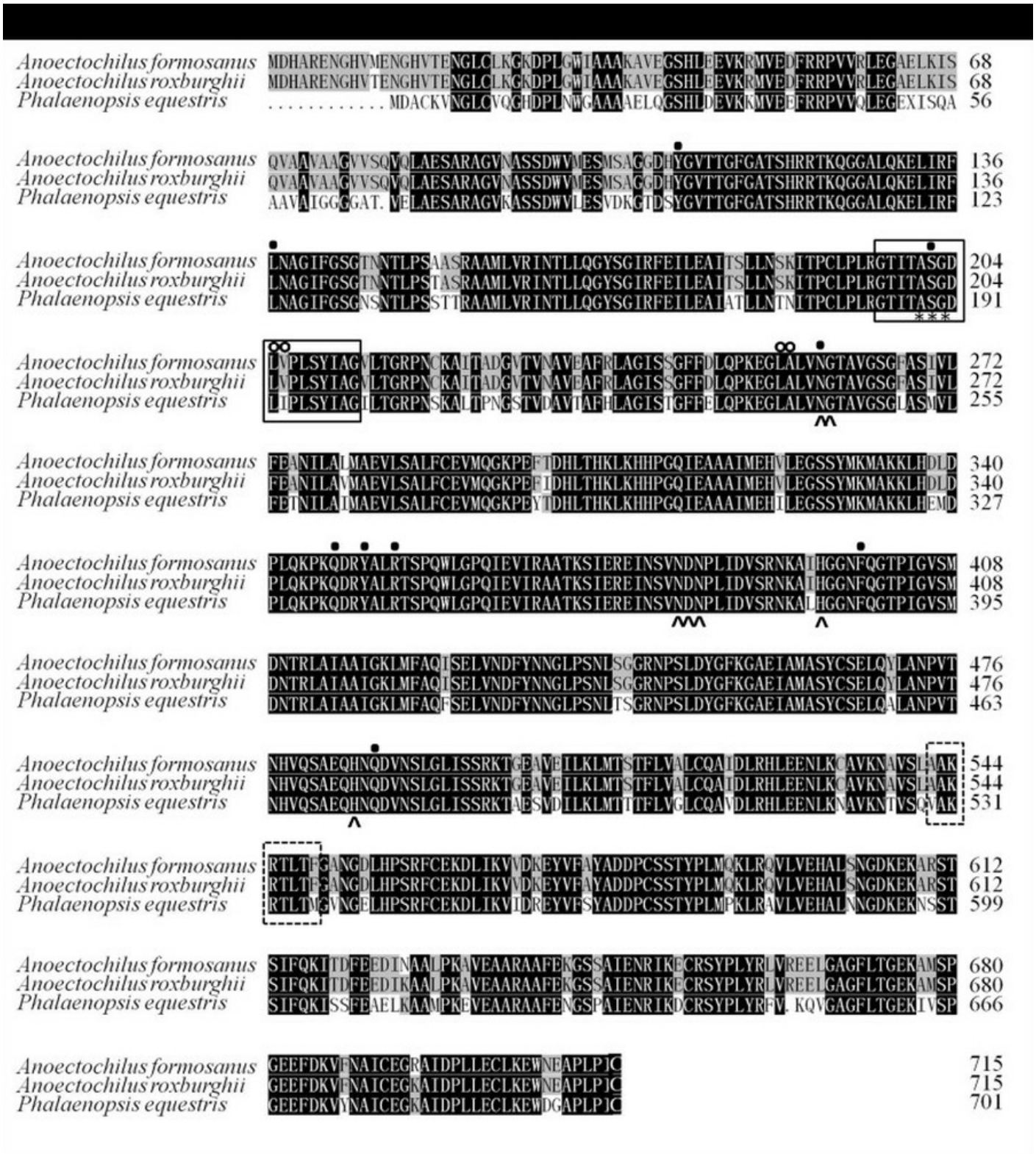
Anoectochilus formosanus
Anoectochilus roxburghii
Phalaenopsis equestris

Figure 3

Figure 3 Phylogenetic tree among the putative proteins of *A. roxburghii*, *A. formosanus* and deposited functional PAL proteins of other plants.

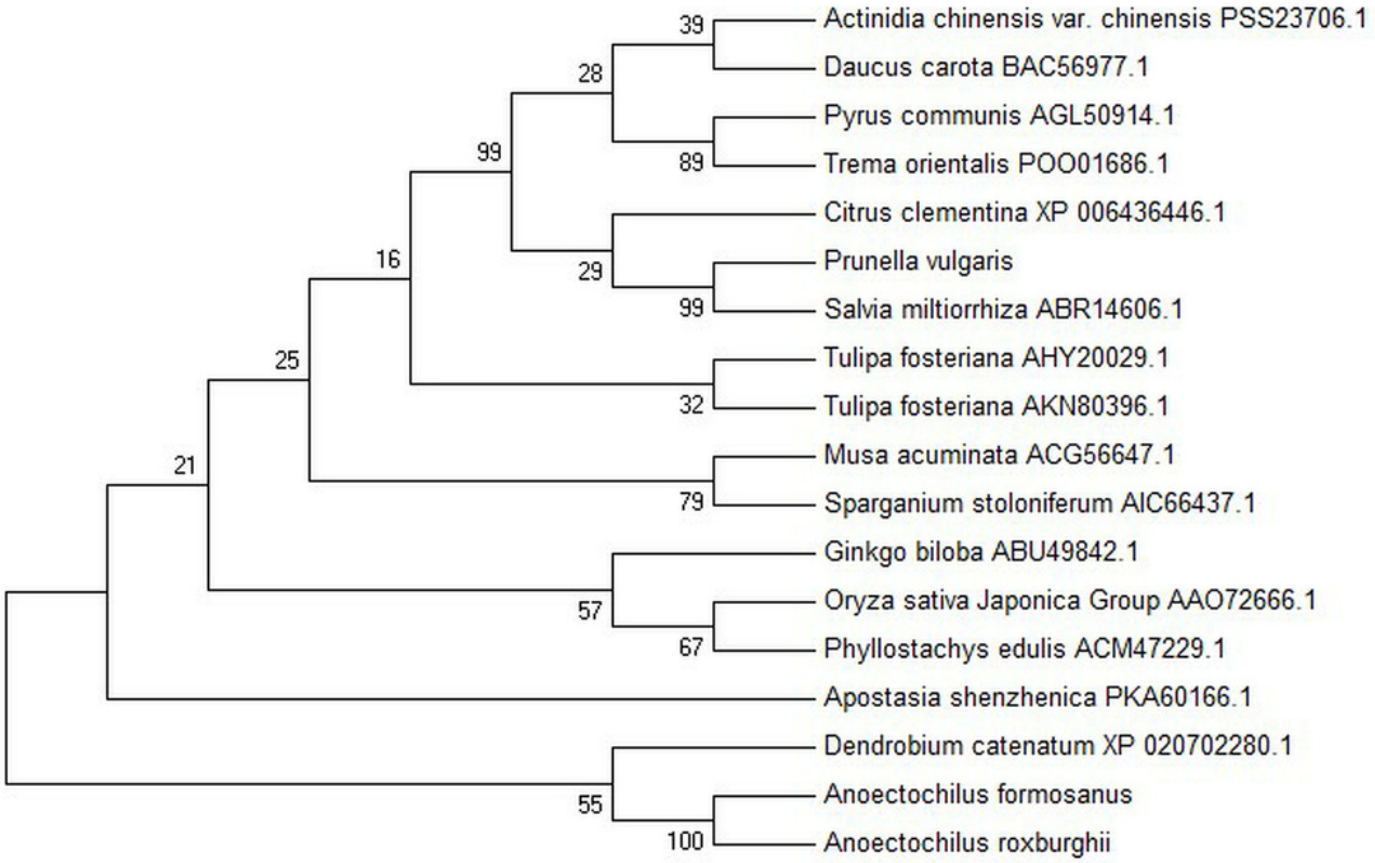

Figure 4

Figure 4 Relative expression levels of *AfPAL* and *ArPAL*genes among different organs.

The darker columns represent *A. formosanus*, the lighter columns represent *A. roxburghii*. The asterisk (*) and double asterisk (**) stand for significance with the control at 0.05 and 0.01 levels, respectively.

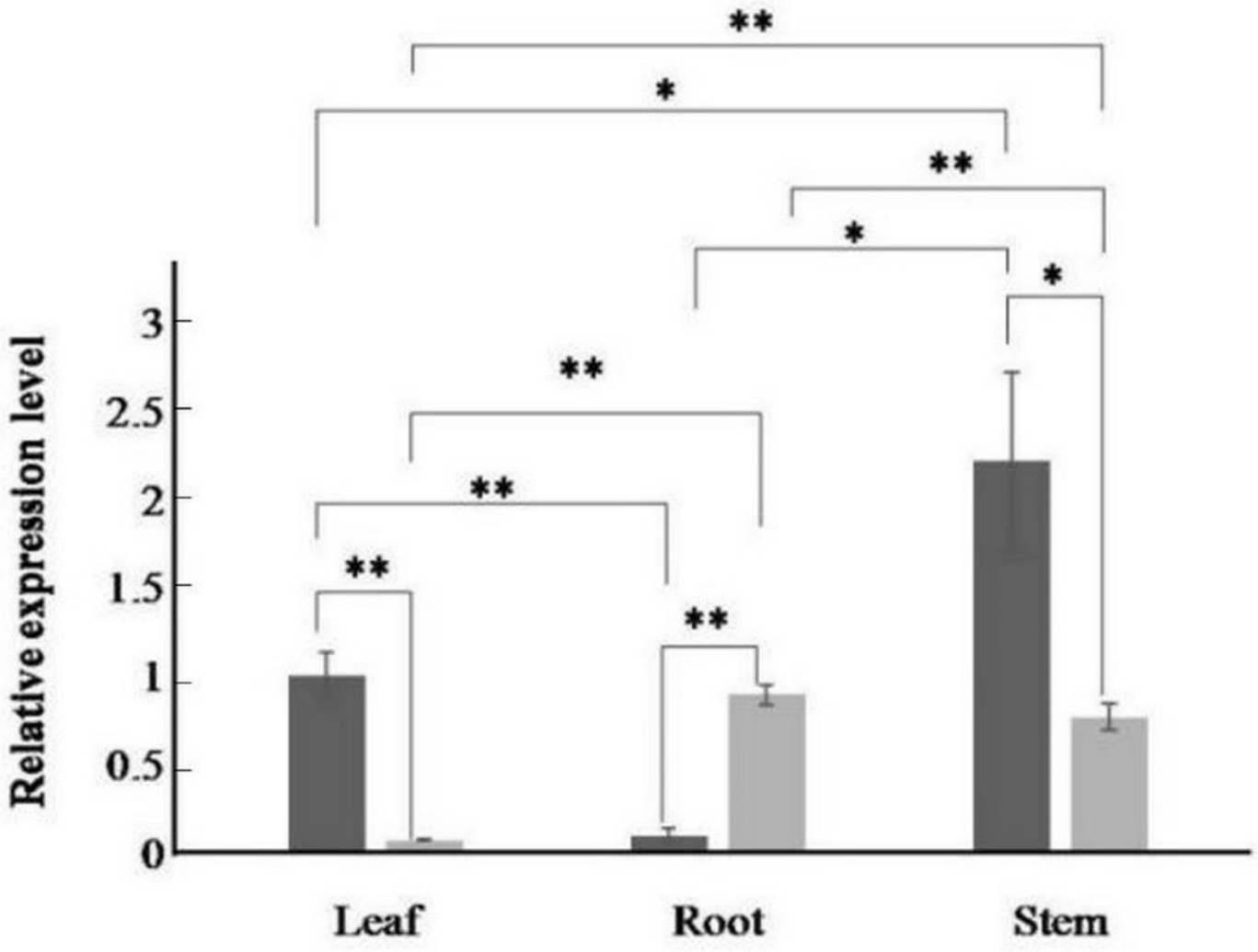

Figure 5

Figure 5 Relative expression level of the *PAL* gene under the stress in *A. formosanus* and *A. roxburghii*.

A: under the Phe stress; B: under the NaCl stress; C: under the UV; D: under the red-light stress. The asterisk (*) and double asterisk (**) stand for significance with the control at 0.05 and 0.01 levels, respectively.

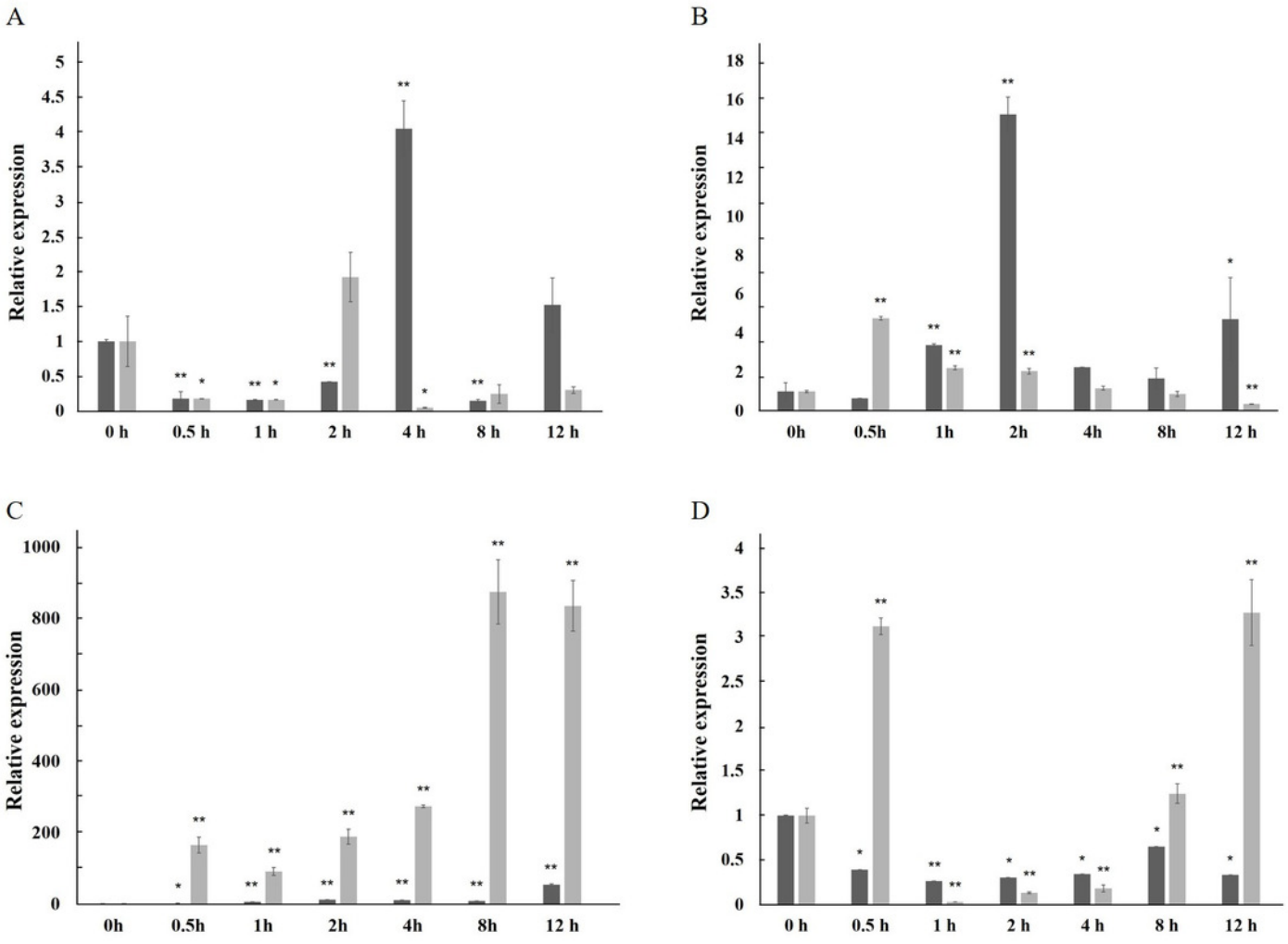

Figure 6

Figure 6 Subcellular localization of PAL protein.

eGFP and *PAL–eGFP* fusion gene were driven under the control of the CaMV 35 Spromoter. A: Epidermal cells of onion transformed by pC2300–*35S–eGFP*. B: Epidermal cells of onion transformed by pC2300–*35S–PAL–eGFP* from *A. formosanus*. C: Epidermal cells of onion transformed by pC2300–35S–PAL–eGFP from *A. roxburghii.*

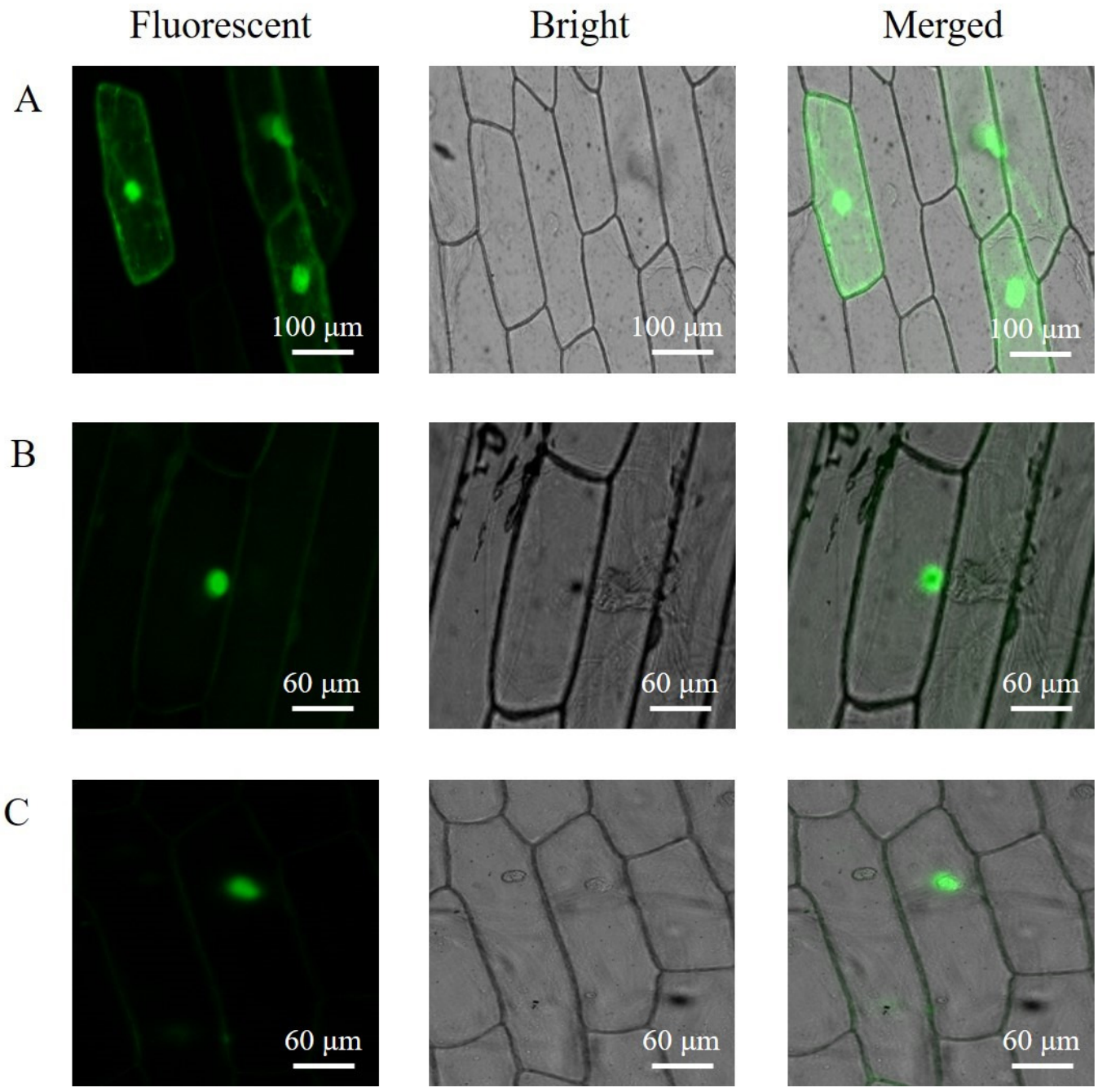
Fluorescent
Bright
Merged
A
100 μm
100 μm
100 μm
B
60 μm
60 μm
60 μm
C
60 μm
60 μm
60 μm

Figure 7

Figure 7 Relative content of total flavonoids and anthocyanin of T3 *Arabidopsis* lines of gene *PAL* from *A. formosanus* and *A. roxburghii*.

A: Relative content of total flavonoids of T3 *Arabidopsis* lines of gene *PAL* from *A. formosanus* and *A. roxburghii*. B:Relative content of anthocyanin of T3 *Arabidopsis* lines of gene *PAL* from *A. formosanus* and *A. roxburghii*. The asterisk (*) and double asterisk (**) stand for significance with the control at 0.05 and 0.01 levels, respectively.

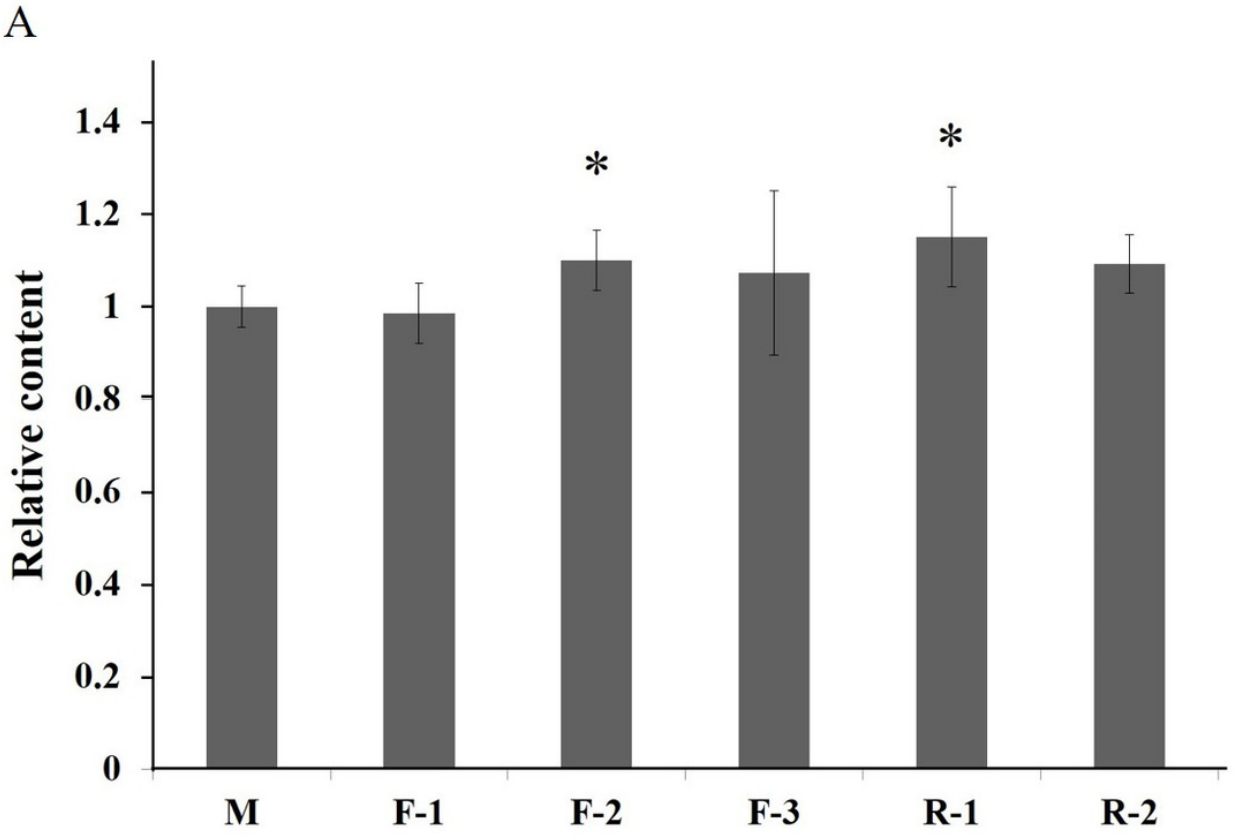
A
Relative content
1.4
1.2
1
0.8
0.6
0.4
0.2
0
*
*
M
F-1
F-2
F-3
R-1
R-2

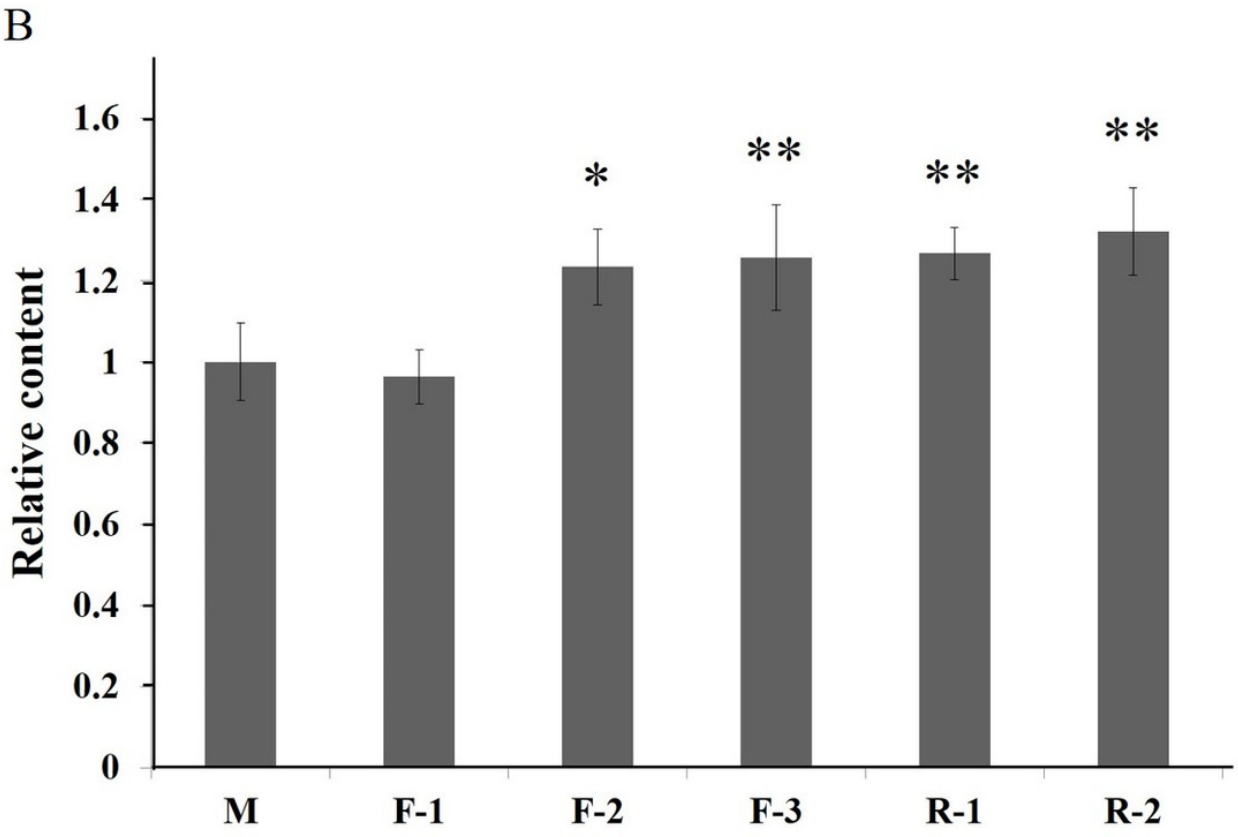
B
Relative content
1.6
1.4
1.2
1
0.8
0.6
0.4
0.2
0
*
**
**
**
M
F-1
F-2
F-3
R-1
R-2